Published in final edited form as:
Cell Calcium. 2014 September ; 56(3): 235–243. doi:10.1016/j.ceca.2014.07.011.

Regulation of endogenous and heterologous Ca^{2+} release-activated Ca^{2+} currents by pH*

Andreas Beck[1,2], **Andrea Fleig**[1], **Reinhold Penner**[1], and **Christine Peinelt**[1,3]

[1]Queen's Center for Biomedical Research, Laboratory of Cell and Molecular Signaling, The Queen's Medical Center, and John A. Burns School of Medicine, University of Hawaii, Honolulu, HI 96813, US

[2] Department of Pharmacology and Toxicology, ZHMB, Saarland University, D-66421 Homburg, Germany

[3] Department of Biophysics, Saarland University, ZHMB, 66421 Homburg, Germany

Abstract

Deviations from physiological pH (~ pH 7.2) as well as altered Ca^{2+} signaling play important roles in immune disease and cancer. One of the most ubiquitous pathways for cellular Ca^{2+} influx is the store-operated Ca^{2+} entry (SOCE) or Ca^{2+} release-activated Ca^{2+} current (I_{CRAC}), which is activated upon depletion of intracellular Ca^{2+} stores. We here show that extracellular and intracellular changes in pH regulate both endogenous I_{CRAC} in Jurkat T lymphocytes and RBL2H3 cells, and heterologous I_{CRAC} in HEK293 cells expressing the molecular components STIM1/2 and Orai1/2/3 (CRACM1/2/3). We find that external acidification suppresses, and alkalization facilitates IP_3-induced I_{CRAC}. In the absence of IP_3, external alkalization did not elicit endogenous I_{CRAC} but was able to activate heterologous I_{CRAC} in HEK293 cells expressing Orai1/2/3 and STIM1 or STIM2. Similarly, internal acidification reduced IP_3-induced activation of endogenous and heterologous I_{CRAC}, while alkalization accelerated its activation kinetics without affecting overall current amplitudes. Mutation of two aspartate residues to uncharged alanine amino acids (D110/112A) in the first extracellular loop of Orai1 significantly attenuated both the inhibition of I_{CRAC} by external acidic pH as well as its facilitation by alkaline conditions. We conclude that intra- and extracellular pH differentially regulates I_{CRAC}. While intracellular pH might affect aggregation and/or binding of STIM to Orai, external pH seems to modulate I_{CRAC} through its channel pore, which in Orai1 is partially mediated by residues D110 and D112.

To whom correspondence should be addressed: Christine Peinelt, Department of Biophysics, ZHMB, Saarland University, 66421 Homburg, Germany, Tel.: (06841) 16-26453; Fax: (06841) 16-26060; (bpcpei@uks.eu) or Reinhold Penner, Laboratory of Cell and Molecular Signaling, The Queen's Medical Center, Honolulu, HI 96813, US, Tel.: (808) 585-5366; Fax: (808) 585-5377; rpenner@hawaii.edu.

Keywords

STIM; Orai; HEK293; Jurkat cells; RBL; whole-cell patch clamp; I_{CRAC}

1. INTRODUCTION

Both, Ca^{2+} signaling and pH are altered in different pathophysiological circumstances such as immune disease and cancer [1-5]. In this context, the pH dependence of Ca^{2+}-permeable ion channels is of particular interest since they are the main provider of the key intracellular second messenger Ca^{2+}. All Ca^{2+} channels examined so far seem to share the same basic pH responsiveness: extracellular acidification reduces and alkalization increases the amplitude of Ca^{2+} inward currents [6-8]. For the L-type voltage-gated Ca^{2+} channel it is suggested that the molecular basis for the effect of extracellular pH changes is a protonation site that lies within the pore and which is formed by a combination of conserved glutamate residues [9]. However, for most pH-dependent effects on Ca^{2+} channels, the underlying mechanisms are not well understood and might differ from each other.

One universally present Ca^{2+} influx mechanism in mammalian cells is the store-operated Ca^{2+} entry (SOCE) [10]. STIM1 and Orai1 (CRACM1) were identified as main molecular components of SOCE and the underlying Ca^{2+} release-activated Ca^{2+} current (I_{CRAC}) [11-16]. Upon store depletion, the endoplasmic reticulum Ca^{2+} sensor STIM1 aggregates and translocates into junctional structures close to the plasma membrane where it binds and activates Orai1, Ca^{2+}-selective ion channels, that have been described as either a tetramer or a hexamer [17-25]. Besides STIM1 and Orai1, the isoforms STIM2, Orai2 and Orai3 are ubiquitously expressed and can form functional channels with distinct biophysical and pharmacological properties [26-33].

Various Ca^{2+} imaging studies have demonstrated that an acidic pH can contribute to lowered SOCE signals in several cell types [34-39]. All these studies show that extracellular acidification decreases and alkalization increases SOCE. Patch-clamp studies of I_{CRAC} corroborate the Ca^{2+} imaging results. I_{CRAC} in human monocyte-derived macrophages shows an extracellular pH-dependent change of current amplitude with a pK_a of 8.2 [40]. Two studies in Jurkat T lymphocytes suggest that extracellular pH modifies the mitochondrial control of SOCE in Jurkat cells [41,42]. Others predict a similar mechanism as assumed for L-type Ca^{2+} channels via the protonation of negatively charged glutamate residues close to the channel pore [43,44]. The glutamate residue E106, which is known to contribute to the selectivity filter of multimeric Orai1 channels [45-47], appears to be involved in the pH dependence of heterologously expressed STIM1/Orai1 CRAC channels [48]. Mutation of E106 to aspartic acid in Orai1 (E106D) resulted in a reverse pH dependence compared to Orai1 wild type: while Orai1 is normally blocked upon external acidification, Orai (E106D) exhibits an increase in inward current at pH 5.1. Hence, protonation of the E106 residue might change the pore size and also Ca^{2+} binding inside the pore, resulting in a block of Orai1.

So far, most of the information regarding pH effects on SOCE or I_{CRAC} has been gathered by Ca^{2+} imaging experiments from diverse cell types or from experiments with heterologous

co-expression of Orai1 and STIM1. Here, we investigate and compare the effects of external and internal pH on the diverse combinations of heterologous STIM/Orai mediated I_{CRAC} in HEK293 ells, and endogenous I_{CRAC} in the RBL2H3 mast cell line and Jurkat T lymphocytes.

2. RESULTS

2.1 Extracellular pH modulates endogenous I_{CRAC}

To study the effects of extracellular pH on endogenous I_{CRAC} in RBL2H3 cells and Jurkat T lymphocytes, I_{CRAC} was first activated via IP_3 in the patch pipette at an external pH of 7.2 and then bath solutions of different pH were applied after I_{CRAC} had fully developed. Figures 1A and B show, that for both cell types the amplitude of I_{CRAC}, measured at -80 mV, increased upon external alkalization (Fig. 1A) and decreased upon external acidification (Fig. 1B). For quantitative analysis of the pH-dependent current changes, all single cell currents were normalized to cell size (pA/pF) and to the amplitude of the inward current right before pH change (here I/I_{120s}), and then averaged (see Fig. 1C for RBL2H3 cells; upper traces show the outward currents). Finally, the relative changes of the inward current (I_{CRAC}; I/I_{120}) amplitudes were plotted versus the external pH (Fig. 1D). A double dose-response equation (see Material and Methods) best represented the dose (pH) response (I/I_{120}) relationships, and the corresponding fits revealed a pK_a (for acidification) of 6.8 and pK_b (for alkalization) of 8.0 for Jurkat T lymphocytes, and a pK_a of 6.7 and pK_b of 7.8 for RBL2H3 cells (Fig. 1D). Changing to external pH 6.0 inhibited I_{CRAC} by more than 80% in both cell types, whereas pH 8.4 increased inward currents in RBL2H3 cells about 24% and in Jurkat T lymphocytes about 80% (Fig. 1D). Outward currents were not significantly affected except for a small current increase of less than 0.5 pA/pF during alkalization (see Figs. 1C, E and F). Figures 1E and F show the inwardly rectifying I/V relationships typical for the Ca^{2+}-selective I_{CRAC} at different external pH from RBL2H3 cells and Jurkat T lymphocytes, respectively. However, in Jurkat T lymphocytes the current at pH 8.4 exhibits a small outward component which might be due to an alternative channel more prevalent in Jurkat T lymphocytes than in RBL2H3 cells.

2.2 pH effects on heterologously expressed STIM/Orai-mediated I_{CRAC} in HEK293 cells

In order to investigate whether heterologous expression of STIM1/2 and Orai1-3 molecules exhibit the same pH dependency as endogenous I_{CRAC} in RBL2H3 and Jurkat T lymphocytes, we transfected Orai1, Orai2 and Orai3 into HEK293 cells stably expressing STIM1 or STIM2. Cells were used 24 to 48 hours after transfection. In analogy to the experiments shown in Fig. 1, bath solutions of pH 6.0, 6.6, 7.8, 8.4 and 9.0 were applied after full development of IP_3-induced I_{CRAC} at 120 s. Fig. 2A shows the pH-dependent changes of I_{CRAC} amplitudes in STIM1/Orai1-expressing HEK293 cells (S1O1), Fig. 2B for STIM1/Orai2 (S1O2), and Fig. 2C for STIM1/Orai3 (S1O3). Plotting the relative pH-dependent current changes (I/I_{120s}) versus the corresponding external pH, revealed similar acidification-dependent decreases of I_{CRAC} in S1O1-, S1O2- and S1O3-expressing HEK293 cells (Fig. 2D) as those observed for endogenous I_{CRAC} in RBL2H3 cells and Jurkat T lymphocytes (see Fig. 1D). However, I_{CRAC} in S1O1-, S1O2- and S1O3-expressing HEK293 cells was more amplified upon alkalization (up to 300%, Fig. 2D) than endogenous

I_{CRAC} in RBL2H3 and Jurkat T lymphocytes (up to ~120% - 180%) (Fig. 1D). The same double dose-response equation as used in Fig. 1D was used to fit the dose-response relationships in Fig. 2D. The pK_a (acidification) and pK_b (alkalization) for S1O1- and S1O2-expressing HEK293 cells (both pK_a 6.8, pK_b 7.9) were comparable to pK_a and pK_b for endogenous I_{CRAC} in RBL2H3 cells and Jurkat T lymphocytes (see above). S1O3-expressing HEK293 cells (pK_a 6.7, pK_b 8.4) revealed a slightly higher pK_b. Fig. 2F shows the typical inwardly rectifying I/V relationships for I_{CRAC} in S1O1-, S1O2-, and S1O3-expressing HEK293 cells at external pH 7.2 (upper curves) and 8.4 (lower curves). As seen in RBL2H3 and Jurkat T lymphocytes, small outward currents appeared during external alkalization (see I/Vs in Fig. 2F).

Under physiological conditions I_{CRAC} is a highly selective Ca^{2+} current. To exclude pH-dependent changes in ion selectivity we replaced the external monovalent cation Na^+ by the ion channel-impermeable cation tetraethylammonium (TEA^+). Na^+-free conditions did not prevent the massive alkalization-induced current increase (Fig. 2E). In addition, no further outward current appeared after external alkalization (see Fig. 2E upper traces and I/Vs in Fig. 2F). This suggests that the alkalization-mediated current increase in STIM1/Orai1-expressing cells is due to an increased Ca^{2+} influx and not to a change in ion selectivity.

Similar to STIM1, STIM2 also mediates large I_{CRAC} currents. When co-expressed with Orai1-3 STIM2 mediates a store-dependent (first phase – fast, small amplitude) and store-independent (second phase – slow, high amplitude) mode of CRAC channel activation [28]. We transiently expressed Orai1 and Orai3 into HEK293 cells stably expressing STIM2 to see whether STIM2-mediated I_{CRAC} shows the same alkalization-induced increase as seen for STIM1. As previously shown, IP_3-induced I_{CRAC} in STIM2/Orai1 (S2O1)-expressing cells produced a significantly larger second-phase current than STIM2/Orai3 (S2O3)-expressing HEK293 cells (Figs. 2G and H; filled circles). External alkalization resulted in an increase of current in both S2O1- and S2O3-expressing cells (Figs. 2G and H; open circles). Fig. 2I illustrates the I/V relationships of IP_3-induced I_{CRAC} in S2O1- and S2O3-expressing HEK293 cells at external pH 7.2 and 8.4. As already observed in IP_3-induced STIM1-mediated I_{CRAC}, outward currents were largely unaffected by external alkalization. Figures 2G and 2H show that the alkalization-induced current potentiation in S2O1- and S2O3-expressing HEK293 cells increased along with the rising secondary phase of I_{CRAC}, and, after applying pH 7.2, the current amplitude declined quickly to levels of control cells (without pH change). This suggests that the alkalization-dependent potentiation of S2O1-mediated I_{CRAC} seems to somehow boost activated open channels, rather than recruiting further closed channels.

Wild type HEK293 cells (HEK wt) and HEK293 cells just expressing Orai1-3, all reveal IP_3- induced I_{CRAC} currents at a basal pH of 7.2 of maximally 1 pA/pF (see supplementary Fig. 1). Alkalization (pH 8.4) increased endogenous IP_3-induced I_{CRAC} in HEK wild type cells about 65%,in Orai1- and Orai2-expressing HEK293 cells about 130%, and in Orai3-expressing cells about 320% (Fig. S1A, I/Vs in Fig. S1B and S1C). The relative increase of current is comparable to the alkalization-mediated increase of IP_3-induced I_{CRAC} in STIM/Orai-expressing HEK293 cells, but the absolute current amplitudes are substantially smaller. This suggests, that after store-depletion only Orai channels, which are stimulated by STIM

are boosted by extracellular alkalization, and additional Orai channels do not open upon extracellular alkalization without contribution of STIM, which is limited in Orai1-3-expressing HEK293 cells.

2.3 Induction of heterologous I_{CRAC} upon extracellular alkalization

The previous experiments assessed the effect of extracellular pH on I_{CRAC} that was already activated by IP_3-induced store depletion. In the next set of experiments, no IP_3 was added to the intracellular solution of the patch pipette. Instead, the intracellular Ca^{2+} concentration was buffered to 150 nM to prevent passive store depletion and thus activation of I_{CRAC}. Under these conditions, RBL2H3, Jurkat T lymphocytes, HEK293 wt cells or HEK293 cells expressing Orai1, Orai2 or Orai3 do not develop $I_{CRAC.}$ Extracellular alkalization (pH 8.4) evoked a small linear current (Figs. 3A and B; I/Vs are shown in 3D and E), which was largest in Orai1- and Orai2-expressing HEK293 and RBL2H3 cells, but still less than 1.5 pA/pF. Only Orai3-expressing HEK293 cells revealed a small current with an inward rectifying I/V-relationship, but this current was also much smaller than in the presence of pH 8.4 after store depletion (Fig. S1). These experiments support our previous findings (see above) that Orai molecules forming the CRAC channels are not directly activated by extracellular alkalization. However, the additional expression of STIM1/2 in Orai1-3-expressing HEK293 cells changed the response to alkalization: without apparent store-depletion, extracellular alkalization induced large I_{CRAC} in S1O1-, S1O2-, S1O3- and S2O1-expressing HEK293 cells (Figs. 3C and F; Fig. S2A-E). The EC_{50} for alkalization induced I_{CRAC} in S1O1-expressing HEK293 cells is 7.8 (Fig. 3I).

In analogy to the electrophysiological results, imaging experiments revealed no Ca^{2+} influx upon application of pH 8.4 onto intact Fura-2 AM loaded RBL2H3 and only a weak intracellular Ca^{2+} increase in HEK wt cells (Fig. 3G). In contrast, pH 8.4 induced a significant Ca^{2+} increase in Jurkat T lymphocytes, which was prevented in the absence of external Ca^{2+} (Fig. 3H). This demonstrates that the application of external pH 8.4 did not result in store depletion, whereas control application of thapsigargin did (Fig. 3H). Consistent with the patch-clamp results and activation of inward currents, S1O2-, S1O3- and S2O1-expressing HEK293 cells also revealed an increase in intracellular Ca^{2+} upon extracellular alkalization, which depended on extracellular Ca^{2+} (Fig. S2F).

2.4 Intracellular effects of pH on endogenous and STIM1/Orai1-mediated I_{CRAC}

We next studied the effect of intracellular pH on IP_3-induced I_{CRAC} in S1O1-expressing HEK293 cells (Figs. 4A and C), RBL2H3 cells (Figs. 4B and C) and Jurkat T lymphocytes (Fig. 4C). Intracellular acidification inhibited IP_3-induced I_{CRAC}, whereas intracellular alkalization did not significantly change its amplitude (Figs. 4A and–C). Upper traces in Fig. 4A and B show the outward currents. The dose (pH) - response (I) relationships of intracellular pH on I_{CRAC} are summarized in Fig. 4C. The mean currents at different intracellular pH were normalized to the maximum current for each cell type. Sigmoidal fits revealed a pK of 6.7 for S1O1-expressing HEK293 cells, 6.4 for RBL2H3 cells and 6.2 for Jurkat T lymphocytes. At an intracellular pH of 6.0 no significant I_{CRAC} could be detected in any cell type. To see whether pH 6.0 inhibited I_{CRAC} due to a pH-dependent inhibition of store depletion via IP_3 we applied 2 μM ionomycin to deplete intracellular Ca^{2+} stores

independently of IP_3 (Fig. 4D). The application of ionomycin did not activate any additional current in S1O1-expressing HEK293 cells, RBL2H3 cells and Jurkat T lymphocytes treated with intracellular IP_3 at an intracellular pH of 6.0 (Fig. 4D).

Since intracellular alkalization did not change the amplitude of IP_3-induced I_{CRAC} we further studied whether intracellular alkalization had any effect on its extracellular alkalization-induced potentiation. Fig. 4E shows, that the potentiation of IP_3-induced I_{CRAC} by an external application of pH 8.4 at an internal pH of 7.2 and 8.4 was not different in S1O1-expressing HEK293 cells. Neither was the relative acidification-induced (pH 6.0) inhibition of IP_3-induced I_{CRAC} in the presence of internal pH 7.2 and 9.0 (Fig. 4F). However, the IP_3-induced I_{CRAC} in S1O1- expressing HEK293 cells and RBL2H3 cells developed faster at alkalized intracellular conditions (see also Figs. 4A, B, E and F).

2.5 Mutations of D110/112A in Orai1 changes its pH profile

Close to the glutamate residue in position 106 (E106), which has already been shown to mediate some pH dependence [48], the first extracellular loop of Orai1 reveals two additional negatively charged residues: aspartate residues D110 and D112. An Orai1 construct in which these two aspartates were mutated to uncharged alanine residues (D110/112A) demonstrated that these residues contribute to the ion selectivity and to the anomalous mole-fraction behavior of Orai1 channels [46]. We tested for the pH dependence of I_{CRAC} via $Orai1_{D110/112A}$ compared to $Orai1_{wt}$. We applied pH 6.0 or pH 8.4 after IP_3-activated I_{CRAC} had developed in HEK293 cells stably expressing STIM1 and either $Orai1_{wt}$ or $Orai1_{D110/112A}$. Currents were normalized to IP_3- induced currents at t=120 s and plotted vs. time (Fig. 5A, I/Vs are shown in 5B). Fig. 5C demonstrates that the alkalization-induced amplification of I_{CRAC} upon application of pH 8.4 was significantly smaller in $Orai1_{D110/112A}$ compared to $Orai1_{wt}$ (Fig. 5C). In addition, the bar diagram in Fig. 5D demonstrates that the residual current upon pH-induced block (pH 6.0) was significantly larger in $Orai1_{D110/112A}$ compared to $Orai1_{wt}$.

3. DISCUSSION

In the present study we assessed extra- and intracellular pH changes on the development and amplitude of the Ca^{2+} release-activated Ca^{2+} current (I_{CRAC}) in HEK293 cells heterologously expressing STIM and Orai proteins and endogeneous I_{CRAC} in RBL2H3 cells as well as Jurkat T lymphocytes.

In agreement with previous studies investigating extracellular pH effects on store-operated Ca^{2+} entry (SOCE) via fluorescent Ca^{2+} imaging [34-39] and/or I_{CRAC} via electrophysiological techniques [40] we found that extracellular acidification decreases and alkalization increases I_{CRAC} in endogenous cells as well as in STIM/Orai co-overexpressing HEK cells (S1O1, S1O2, S1O3, S2O1, S2O3). Since the pH/current relationships reveal very similar pKs for acidification-induced inhibition (6.7-6.8) and pKs for alkalization-induced potentiation (7.8-8.4) in both endogenous and heterologously expressed I_{CRAC}, we assume that the extracellular pH dependency is a general feature of I_{CRAC}. In RBL2H3 cells and Jurkat T lymphocytes the differences in pK values might result from different expression levels of STIM and Orai homologues.

Recently, the glutamate residue E106 in Orai1 has been identified to contribute to the extracellular pH dependence of Ca^{2+} release-activated Ca^{2+} (CRAC) channels [48]. Here, we demonstrate that two aspartate residues in the first extracellular loop of Orai1, close to E106, also contribute to the pH-induced changes of I_{CRAC}. The lower degree of amplification of $Orai1_{D110/112A}$ could be explained by the absence of negative charges, resulting in a missing energy-well for the Ca^{2+} coordination of the first loop close to the ion channel pore. In conclusion a protonation of D110/112 could decrease current size at low pH. The less efficient block of $Orai1_{D110/112A}$ at low pH is possibly due to changed steric arrangement of the uncharged alanine residues compared to the protonated aspartate residues probably increasing Orai channel conductance.

Extracellular alkalization of Orai1-3 in the absence of STIM did not result in a substantial increase of CRAC currents. This suggests that the potentiation by extracellular pH only affects Orai channels that interact with STIM. However, I_{CRAC} and Ca^{2+} influx in HEK293 cells co-overexpressing different STIM and Orai combinations as well as Ca^{2+} influx in Jurkat T lymphocytes can be activated by extracellular alkalization without apparent store-depletion. Taken together, our data suggest that extracellular alkalization can activate I_{CRAC} in the STIM/Orai overexpression system, but apparently no endogenous I_{CRAC}. Since no alkalization-mediated endogenous I_{CRAC} was detectable in HEK wt, RBL and Jurkat T lymphocytes, it remains unclear whether the alkalization-mediated Ca^{2+} influx in Jurkat T lymphocytes depends in endogenous STIM/Orai channels, or is mediated via other Ca^{2+} influx pathways in these cells.

Intracellular pH also affects I_{CRAC}. Our results show that intracellular acidification inhibits both endogenous and heterologous I_{CRAC}, while intracellular alkalization did not alter the current amplitude. The internal pH-dependent inactivation of I_{CRAC} in RBL cells correlates with a pH-dependent inactivation of $iPLA_2\beta$ [49], which is already shown to be a modulator of I_{CRAC} [50]. However, in human neuroblastoma cells, intracellular changes in pH left carbachol-induced Ca^{2+} entry unaffected [35]. Since we induced store-depletion by IP_3 already in the presence of the diverse pH concentrations in the patch pipette, the decrease in I_{CRAC} activation at a lower intracellular pH might be due to an acidic-pH-dependent inhibition of IP_3 binding to its receptor in the membrane of the endoplasmic reticulum, resulting in a slower Ca^{2+} store depletion und thus I_{CRAC} activation [51]. However, a further IP_3 receptor-independent induction of store depletion by the Ca^{2+} ionophore ionomycin did not result in the CRAC currents at an intracellular pH of 6.0 either. These results imply that intracellular acidification directly blocks the STIM/Orai machinery. This concept is supported by two recent studies. Investigations of reduced SOCE in human alveolar smooth muscle cells upon hypoxia-induced intracellular acidification and I_{CRAC} in HEK293 cells heterologously expressing STIM1 and Orai1 suggest an uncoupling of STIM1 and Orai1 due the intracellular drop of pH, which might be an important mechanism to protect cells from Ca^{2+} overload under hypoxic stress [52]. In addition, experiments with STIM1 siRNA in pheochromocytoma cells demonstrate that changes in pH alter the ability of STIM1 to trigger SOCE either due to inhibition of conformational changes or decreased STIM1 translocation or aggregation [53].

Several publications discuss a reduced or increased store-operated Ca^{2+} entry along with cancer- E.g., lowered SOCE-conducted Ca^{2+} signaling can result in typical cancer hallmark functions such as enhanced proliferation, inability to induce apoptosis and a higher migration potential [54-56]. Tumor environment is often characterized by an acidic pH [57] and various chemical and technical approaches use acidic tumor environment to unfold their therapeutic potential [58-61]. Recent work demonstrated a role for STIM/Orai isoforms STIM2 and Orai3 in the pathophysiology of cancer [62-69]. Our results imply that low pH in tumor environment might contribute to low SOCE signaling.

In addition, the strong external pH-sensitivity might be of physiological significance in the activation of immune cells. Low extracellular pH can contribute significantly to the modulation of SOCE in cells at sites of inflammation. In the microenvironment of abscesses, the external pH can be as low as 5.5 [70] and acidic microenvironments may play a role in inhibiting immune function as suggested to be the case in cystic fibrosis [71]. The acidification-induced inhibition of I_{CRAC}, most probably one of the most important factors in immune cell activation, might well be the reason for the well-known diminished immune response at lowered extracellular pH. However, the reduction of Ca^{2+} influx in acidic environment may also be an intrinsic protective feedback mechanism in inflammatory cells.

CONCLUSION

In cancer and immune reaction extracellular pH is lowered and Ca^{2+} signals are impaired. Endogenous and STIM/Orai mediated I_{CRAC} depend on intra- and extracellular pH and two aspartic acids in the pore of Orai1 contribute to the extracellular pH-dependence. Inhibition of Ca^{2+} influx via Orai channels upon extracellular acidification is a general feature of I_{CRAC} and lowered pH in tumors and immune response can thus contribute to Ca^{2+} dependent malfunctions.

4. MATERIAL AND METHODS

4.1 Cells

HEK293 wild type (wt) and stably expressing STIM1 or STIM2 cells [72] were cultured at 37°C with 5% CO_2 in DMEM supplemented with 10% fetal bovine serum (FBS). Before experiments, STIM2-expressing cells were grown for several days or weeks in the absence of G418 (500 μg/ml; see [28]). Full length human Orai1, Orai2 and Orai3 were subcloned into pCAGGS-IRES-GFP for transient dicistronic expression with the green fluorescent protein (GFP) as described previously [27]. For electrophysiological experiments, Orai1, Orai2 and Orai3 proteins were over-expressed in HEK293 wt or stably expressing STIM1 or STIM2 cells using lipofectamine 2000 (Invitrogen). GFP-expressing cells were selected by fluorescence. Experiments were performed 24-48 hours after transfection.

Jurkat T lymphocytes and RBL2H3 cells were cultured at 37°C with 5% CO_2 in RPMI-1640 medium and in DMEM medium, respectively, both supplemented with 10% FBS and 0.1% penicillin-streptomycin.

4.2 Electrophysiology

Patch pipettes, pulled from glass capillaries (inner diameter 1.5 mm, Kimble products) with a horizontal puller (Sutter instruments, Model P-97), were fire-polished, and had resistances between 2 and 4 MΩ. Patch clamp experiments were performed in the tight-seal whole-cell configuration at 21-25 °C. High-resolution current recordings were acquired and analyzed using the EPC-10 and the software PatchMaster (HEKA). Voltage ramps of 50 ms duration spanning a range of −100 to +100 mV (or −150 to +150 mV) were delivered from a holding potential of 0 mV at a rate of 0.5 Hz over a period of 120-600 s. All voltages were corrected for a liquid junction potential of 10 mV. Currents were filtered at 2.9 kHz and digitized at 100 μs intervals. Capacitive currents were determined and corrected before each voltage ramp. Extracting the current amplitude at −80 mV and +80 mV from individual ramp current records assessed the low-resolution temporal development of inward and outward currents, respectively. All currents were normalized to the cell size and displayed as current densities (pA/pF). Standard external solutions contained (in mM): 120 NaCl, 2 $MgCl_2$, 10 $CaCl_2$, 10 TEA-Cl, 10 HEPES, 10 glucose, pH 7.2 with NaOH, 300 mOsm. In some experiments, NaCl was replaced equimolarly by tetraethylammonium-chloride (TEA-Cl). The external solution was set to different pH by adding NaOH or HCl and pressure-applied directly onto the cell of interest via a wide-tipped puffer pipette. If necessary, osmolarity was adjusted by adding sucrose. Standard internal solutions contained (in mM): 120 Cs-glutamate, 20 1,2-bis(2-aminophenoxy)ethane-*N*,*N*,*N*’,*N*’-tetraacetic acid tetracesium salt (Cs-BAPTA), 3 $MgCl_2$, 10 HEPES, 0.02 IP_3, pH 7.2 with CsOH, 300 mOsm. For some experiments IP_3 was omitted and $[Ca^{2+}]_i$ was buffered to 150 nM using 20 mM Cs·BAPTA and 8 mM $CaCl_2$ (8.5 mM for pH 8.4) as calculated with WebMaxC, http://www.stanford.edu/~cpatton/webmaxcS.htm). The intracellular solution was set to different pH by adding CsOH or HCl. All chemicals were purchased from Sigma-Aldrich Co (St. Louis, MO, USA). For some experiments, 2 μM ionomycin (Sigma) was applied extracellularly.

4.3 Fluorescence measurements

For Ca^{2+} measurements, cells were loaded with fura-2 AM (Molecular Probes, Eugene, OR, USA; 1 μM / 60 min / 37 °C) and kept in extracellular saline containing 10 mM $CaCl_2$. External solution of pH 8.4 with or without 10 mM $CaCl_2$ or external solution (pH 7.4) without $CaCl_2$ but 2 μM thapsigargin were applied onto the cell of interest via puffer pipette. Experiments were performed with a Zeiss Axiovert 200 fluorescence microscope equipped with a dual excitation fluorimetric imaging system (TILL-Photonics, Gräfelfingen, Germany), using a 40x Plan NeoFluar objective. Data acquisition and computation were controlled by X-Chart (HEKA). Cells were excited by wavelengths of 360 nm and 390 nm produced by a monochromator B (TILL-Photonics). The fluorescence emission was recorded with a photomultiplier tube (TILL-Photonics) using an optical 440 nm longpass filter. The signals were sampled at 5 Hz and computed into relative ratio units of the fluorescence intensity at the different wavelengths (360/390 nm). Results are given as the approximate $[Ca^{2+}]_i$, calculated from the 360/390 nm fluorescence ratios, using an *in vivo* Ca^{2+} calibration performed in patch-clamp experiments with defined Ca^{2+} concentrations

combined with 200 μM fura-2 pentapotassium salt (Molecular Probes, Eugene, OR, USA) in the patch pipette.

4.4 Statistics and Analysis

Double dose-response equations ($y=y_{mzx1}/1+(pH/pK_a)^{n1}+y_{max2}/1+(pH/pK_b)^{n2}$, $y=I/I_{120s}$, pK_a and n_1 = pK and Hill coefficient for external acidification, and pK_b and n_2 = pK and Hill coefficient for external alkalization) were used to represent the dose (external pH) - response (I/I_{120}) relationships. Sigmoidal fits ($y=y_{max}/1+(pH/pK)^n$, $y=I/I_{max}$, pK and n = Hill coefficient) were used to represent the dose (internal pH) - response (I/I_{120}) relationships. Where applicable, statistical errors of averaged data are given as means ±SEM with n determinations.

Supplementary Material

Refer to Web version on PubMed Central for supplementary material.

Acknowledgments

We thank Mahealani Monteilh-Zoller, Miyoko Bellinger, Angela Love and Stephanie Johne for excellent technical support. Supported in part by NIH grants R01-AI050200 (RP) and Deutsche Forschungsgemeinschaft PE 1478/5-1 (CP) and SFB894 (AB and CP).

REFERENCES

1. Glitsch M. Protons and Ca2+: ionic allies in tumor progression? Physiology (Bethesda). 2011; 26:252–265. [PubMed: 21841073]
2. Lardner A. The effects of extracellular pH on immune function. J Leukoc Biol. 2001; 69:522–530. [PubMed: 11310837]
3. Monteith GR, McAndrew D, Faddy HM, Roberts-Thomson SJ. Calcium and cancer: targeting Ca2+ transport. Nat Rev Cancer. 2007; 7:519–530. [PubMed: 17585332]
4. Cahalan MD, Chandy KG. The functional network of ion channels in T lymphocytes. Immunol Rev. 2009; 231:59–87. [PubMed: 19754890]
5. Shaw PJ, Feske S. Physiological and pathophysiological functions of SOCE in the immune system. Front Biosci (Elite Ed). 2012; 4:2253–2268. [PubMed: 22202035]
6. Iijima T, Ciani S, Hagiwara S. Effects of the external pH on Ca channels: experimental studies and theoretical considerations using a two-site, two-ion model. Proc Natl Acad Sci U S A. 1986; 83:654–658. [PubMed: 2418439]
7. Tombaugh GC, Somjen GG. Effects of extracellular pH on voltage-gated Na+, K+ and Ca2+ currents in isolated rat CA1 neurons. J Physiol. 1996; 493(Pt 3):719–732. [PubMed: 8799894]
8. Smirnov SV, Knock GA, Belevych AE, Aaronson PI. Mechanism of effect of extracellular pH on L-type Ca(2+) channel currents in human mesenteric arterial cells. Am J Physiol Heart Circ Physiol. 2000; 279:H76–85. [PubMed: 10899043]
9. Chen XH, Tsien RW. Aspartate substitutions establish the concerted action of P-region glutamates in repeats I and III in forming the protonation site of L-type Ca2+ channels. J Biol Chem. 1997; 272:30002–30008. [PubMed: 9374474]
10. Lewis RS. Store-operated calcium channels: new perspectives on mechanism and function. Cold Spring Harb Perspect Biol. 2011; 3 10.1101/cshperspect.a003970.
11. Peinelt C, Vig M, Koomoa DL, et al. Amplification of CRAC current by STIM1 and CRACM1 (Orai1). Nat Cell Biol. 2006; 8:771–773. [PubMed: 16733527]
12. Vig M, Peinelt C, Beck A, et al. CRACM1 is a plasma membrane protein essential for store-operated Ca2+ entry. Science. 2006; 312:1220–1223. [PubMed: 16645049]

13. Feske S, Gwack Y, Prakriya M, et al. A mutation in Orai1 causes immune deficiency by abrogating CRAC channel function. Nature. 2006; 441:179–185. [PubMed: 16582901]
14. Zhang SL, Yeromin AV, Zhang XH, et al. Genome-wide RNAi screen of Ca(2+) influx identifies genes that regulate Ca(2+) release-activated Ca(2+) channel activity. Proc Natl Acad Sci U S A. 2006; 103:9357–9362. [PubMed: 16751269]
15. Liou J, Kim ML, Heo WD, et al. STIM is a Ca2+ sensor essential for Ca2+-store-depletion-triggered Ca2+ influx. Curr Biol. 2005; 15:1235–1241. [PubMed: 16005298]
16. Roos J, DiGregorio PJ, Yeromin AV, et al. STIM1, an essential and conserved component of store-operated Ca2+ channel function. J Cell Biol. 2005; 169:435–445. [PubMed: 15866891]
17. Thompson JL, Shuttleworth TJ. How Many Orai's Does It Take to Make a CRAC Channel? Sci Rep. 2013; 3:1961. [PubMed: 23743658]
18. Hou X, Pedi L, Diver MM, Long SB. Crystal structure of the calcium release-activated calcium channel Orai. Science. 2012; 338:1308–1313. [PubMed: 23180775]
19. Ji W, Xu P, Li Z, et al. Functional stoichiometry of the unitary calcium-release-activated calcium channel. Proc Natl Acad Sci U S A. 2008; 105:13668–13673. [PubMed: 18757751]
20. Penna A, Demuro A, Yeromin AV, et al. The CRAC channel consists of a tetramer formed by Stim-induced dimerization of Orai dimers. Nature. 2008; 456:116–120. [PubMed: 18820677]
21. Demuro A, Penna A, Safrina O, et al. Subunit stoichiometry of human Orai1 and Orai3 channels in closed and open states. Proc Natl Acad Sci U S A. 2011; 108:17832–17837. [PubMed: 21987805]
22. Madl J, Weghuber J, Fritsch R, et al. Resting state Orai1 diffuses as homotetramer in the plasma membrane of live mammalian cells. J Biol Chem. 2010; 285:41135–41142. [PubMed: 20961852]
23. Maruyama Y, Ogura T, Mio K, et al. Tetrameric Orai1 is a teardrop-shaped molecule with a long, tapered cytoplasmic domain. J Biol Chem. 2009; 284:13676–13685. [PubMed: 19289460]
24. Wu MM, Buchanan J, Luik RM, Lewis RS. Ca2+ store depletion causes STIM1 to accumulate in ER regions closely associated with the plasma membrane. J Cell Biol. 2006; 174:803–813. [PubMed: 16966422]
25. Luik RM, Wu MM, Buchanan J, Lewis RS. The elementary unit of store-operated Ca2+ entry: local activation of CRAC channels by STIM1 at ER-plasma membrane junctions. J Cell Biol. 2006; 174:815–825. [PubMed: 16966423]
26. Gwack Y, Srikanth S, Feske S, et al. Biochemical and functional characterization of Orai proteins. J Biol Chem. 2007; 282:16232–16243. [PubMed: 17293345]
27. Lis A, Peinelt C, Beck A, et al. CRACM1, CRACM2, and CRACM3 are store-operated Ca2+ channels with distinct functional properties. Curr Biol. 2007; 17:794–800. [PubMed: 17442569]
28. Parvez S, Beck A, Peinelt C, et al. STIM2 protein mediates distinct store-dependent and store-independent modes of CRAC channel activation. FASEB J. 2008; 22:752–761. [PubMed: 17905723]
29. Mercer JC, Dehaven WI, Smyth JT, et al. Large store-operated calcium selective currents due to co-expression of Orai1 or Orai2 with the intracellular calcium sensor. Stim1, J Biol Chem. 2006; 281:24979–24990.
30. Zhang SL, Kozak JA, Jiang W, et al. Store-dependent and -independent modes regulating Ca2+ release-activated Ca2+ channel activity of human Orai1 and Orai3. J Biol Chem. 2008; 283:17662–17671. [PubMed: 18420579]
31. Bogeski I, Al-Ansary D, Qu B, Niemeyer BA, Hoth M, Peinelt C. Pharmacology of ORAI channels as a tool to understand their physiological functions. Expert Rev Clin Pharmacol. 2010; 3:291–303. [PubMed: 22111611]
32. Hoth M, Niemeyer BA. The Neglected CRAC Proteins: Orai2, Orai3, and STIM2. Curr Top Membr. 2013; 71:237–271. [PubMed: 23890118]
33. Frischauf I, Muik M, Derler I, et al. Molecular determinants of the coupling between STIM1 and Orai channels: differential activation of Orai1-3 channels by a STIM1 coiled-coil mutant. J Biol Chem. 2009; 284:21696–21706. [PubMed: 19506081]
34. Zhang Y, Duszynski J, Hreniuk S, Waybill MM, LaNoue KF. Regulation of plasma membrane permeability to calcium in primary cultures of rat hepatocytes. Cell Calcium. 1991; 12:559–575. [PubMed: 1659496]

35. Laskay G, Kalman K, Van Kerkhove E, Steels P, Ameloot M. Store-operated Ca2+-channels are sensitive to changes in extracellular pH. Biochem Biophys Res Commun. 2005; 337:571–579. [PubMed: 16198307]
36. Iwasawa K, Nakajima T, Hazama H, et al. Effects of extracellular pH on receptor-mediated Ca2+ influx in A7r5 rat smooth muscle cells: involvement of two different types of channel. J Physiol. 1997; 503(Pt 2):237–251. [PubMed: 9306269]
37. Weirich J, Dumont L, Fleckenstein-Grun G. Contribution of store-operated Ca2+ entry to pHo-dependent changes in vascular tone of porcine coronary smooth muscle. Cell Calcium. 2004; 35:9–20. [PubMed: 14670367]
38. Marumo M, Suehiro A, Kakishita E, Groschner K, Wakabayashi I. Extracellular pH affects platelet aggregation associated with modulation of store-operated Ca(2+) entry. Thromb Res. 2001; 104:353–360. [PubMed: 11738078]
39. Khoo C, Helm J, Choi HB, Kim SU, McLarnon JG. Inhibition of store-operated Ca(2+) influx by acidic extracellular pH in cultured human microglia. Glia. 2001; 36:22–30. [PubMed: 11571781]
40. Malayev A, Nelson DJ. Extracellular pH modulates the Ca2+ current activated by depletion of intracellular Ca2+ stores in human macrophages. J Membr Biol. 1995; 146:101–111. [PubMed: 7563033]
41. Zablocki K, Szczepanowska J, Duszynski J. Extracellular pH modifies mitochondrial control of capacitative calcium entry in Jurkat cells. J Biol Chem. 2005; 280:3516–3521. [PubMed: 15569668]
42. Zablocki K, Makowska A, Duszynski J. pH-dependent effect of mitochondria on calcium influx into Jurkat cells; a novel mechanism of cell protection against calcium entry during energy stress. Cell Calcium. 2003; 33:91–99. [PubMed: 12531185]
43. Kerschbaum HH, Cahalan MD. Monovalent permeability, rectification, and ionic block of store-operated calcium channels in Jurkat T lymphocytes. J Gen Physiol. 1998; 111:521–537. [PubMed: 9524136]
44. Chen XH, Bezprozvanny I, Tsien RW. Molecular basis of proton block of L-type Ca2+ channels. J Gen Physiol. 1996; 108:363–374. [PubMed: 8923262]
45. Yeromin AV, Zhang SL, Jiang W, Yu Y, Safrina O, Cahalan MD. Molecular identification of the CRAC channel by altered ion selectivity in a mutant of Orai. Nature. 2006; 443:226–229. [PubMed: 16921385]
46. Vig M, Beck A, Billingsley JM, et al. CRACM1 multimers form the ion-selective pore of the CRAC channel. Curr Biol. 2006; 16:2073–2079. [PubMed: 16978865]
47. Prakriya M, Feske S, Gwack Y, Srikanth S, Rao A, Hogan PG. Orai1 is an essential pore subunit of the CRAC channel. Nature. 2006; 443:230–233. [PubMed: 16921383]
48. Scrimgeour NR, Wilson DP, Rychkov GY. Glu(1)(0)(6) in the Orai1 pore contributes to fast Ca(2)(+)-dependent inactivation and pH dependence of Ca(2)(+) release-activated Ca(2)(+) (CRAC) current. Biochem J. 2012; 441:743–753. [PubMed: 21967483]
49. Csutora P, Zarayskiy V, Peter K, et al. Activation mechanism for CRAC current and store-operated Ca2+ entry: calcium influx factor and Ca2+-independent phospholipase A2beta-mediated pathway. J Biol Chem. 2006; 281:34926–34935. [PubMed: 17003039]
50. Smani T, Zakharov SI, Leno E, Csutora P, Trepakova ES, Bolotina VM. Ca2+-independent phospholipase A2 is a novel determinant of store-operated Ca2+ entry. J Biol Chem. 2003; 278:11909–11915. [PubMed: 12547829]
51. Tsukioka M, Iino M, Endo M. pH dependence of inositol 1,4,5-trisphosphate-induced Ca2+ release in permeabilized smooth muscle cells of the guinea-pig. J Physiol. 1994; 475:369–375. [PubMed: 8006822]
52. Mancarella S, Wang Y, Deng X, et al. Hypoxia-induced acidosis uncouples the STIM-Orai calcium signaling complex. J Biol Chem. 2011; 286:44788–44798. [PubMed: 22084246]
53. Thompson MA, Pabelick CM, Prakash YS. Role of STIM1 in regulation of store-operated Ca2+ influx in pheochromocytoma cells. Cell Mol Neurobiol. 2009; 29:193–202. [PubMed: 18807171]
54. Roderick HL, Cook SJ. Ca2+ signalling checkpoints in cancer: remodelling Ca2+ for cancer cell proliferation and survival. Nat Rev Cancer. 2008; 8:361–375. [PubMed: 18432251]

55. Prevarskaya N, Skryma R, Shuba Y. Calcium in tumour metastasis: new roles for known actors. Nat Rev Cancer. 2011; 11:609–618. [PubMed: 21779011]
56. Bergmeier W, Weidinger C, Zee I, Feske S. Emerging roles of store-operated Ca(2)(+) entry through STIM and ORAI proteins in immunity, hemostasis and cancer. Channels (Austin). 2013; 7:379–391. [PubMed: 23511024]
57. Tannock IF, Rotin D. Acid pH in tumors and its potential for therapeutic exploitation. Cancer Res. 1989; 49:4373–4384. [PubMed: 2545340]
58. Amoozgar Z, Park J, Lin Q, Yeo Y. Low molecular-weight chitosan as a pH-sensitive stealth coating for tumor-specific drug delivery. Mol Pharm. 2012; 9:1262–1270. [PubMed: 22489704]
59. Barar J, Omidi Y. Dysregulated pH in Tumor Microenvironment Checkmates Cancer Therapy. Bioimpacts. 2013; 3:149–162. [PubMed: 24455478]
60. Wuang SC, Neoh KG, Kang ET, Leckband DE, Pack DW. Acid-Sensitive Magnetic Nanoparticles as Potential Drug Depots. AIChE J. 2011; 57:1638–1645. [PubMed: 21760639]
61. Lee ES, Gao Z, Bae YH. Recent progress in tumor pH targeting nanotechnology. J Control Release. 2008; 132:164–170. [PubMed: 18571265]
62. Stanisz H, Saul S, Muller CS, et al. Inverse regulation of melanoma growth and migration by Orai1/STIM2-dependent calcium entry. Pigment Cell Melanoma Res. 2014
63. Holzmann C, Kilch T, Kappel S, et al. ICRAC controls the rapid androgen response in human primary prostate epithelial cells and is altered in prostate cancer. Oncotarget. 2013; 4:2096–2107. [PubMed: 24240085]
64. Stanisz H, Stark A, Kilch T, et al. ORAI1 Ca(2+) channels control endothelin-1-induced mitogenesis and melanogenesis in primary human melanocytes. J Invest Dermatol. 2012; 132:1443–1451. [PubMed: 22318387]
65. Motiani RK, Zhang X, Harmon KE, et al. Orai3 is an estrogen receptor alpha-regulated Ca2+ channel that promotes tumorigenesis. FASEB J. 2013; 27:63–75. [PubMed: 22993197]
66. Motiani RK, Abdullaev IF, Trebak M. A novel native store-operated calcium channel encoded by Orai3: selective requirement of Orai3 versus Orai1 in estrogen receptor-positive versus estrogen receptor-negative breast cancer cells. J Biol Chem. 2010; 285:19173–19183. [PubMed: 20395295]
67. Umemura M, Baljinnyam E, Feske S, et al. Store-Operated Ca(2) (+) Entry (SOCE) Regulates Melanoma Proliferation and Cell Migration. PLoS One. 2014; 9:e89292. [PubMed: 24586666]
68. Faouzi M, Hague F, Potier M, Ahidouch A, Sevestre H, Ouadid-Ahidouch H. Down-regulation of Orai3 arrests cell-cycle progression and induces apoptosis in breast cancer cells but not in normal breast epithelial cells. J Cell Physiol. 2011; 226:542–551. [PubMed: 20683915]
69. Faouzi M, Kischel P, Hague F, et al. ORAI3 silencing alters cell proliferation and cell cycle progression via c-myc pathway in breast cancer cells. Biochim Biophys Acta. 2013; 1833:752–760. [PubMed: 23266555]
70. Bryant RE, Fox K, Oh G, Morthland VH. Beta-lactam enhancement of aminoglycoside activity under conditions of reduced pH and oxygen tension that may exist in infected tissues. J Infect Dis. 1992; 165:676–682. [PubMed: 1552196]
71. Bidani A, Wang CZ, Saggi SJ, Heming TA. Evidence for pH sensitivity of tumor necrosis factor-alpha release by alveolar macrophages. Lung. 1998; 176:111–121. [PubMed: 9500296]
72. Soboloff J, Spassova MA, Hewavitharana T, et al. STIM2 is an inhibitor of STIM1-mediated store-operated Ca2+ Entry. Curr Biol. 2006; 16:1465–1470. [PubMed: 16860747]

- I_{CRAC} function depends on intra- and extracellular pH
- Aspartic acids (D110/D112) in Orai1 contribute to the extracellular pH-dependence
- Inhibition of Ca^{2+} influx by low extracellular pH is a general feature of I_{CRAC}
- Low pH in tumors and infection may thus contribute to dysfunctional Ca^{2+} signaling

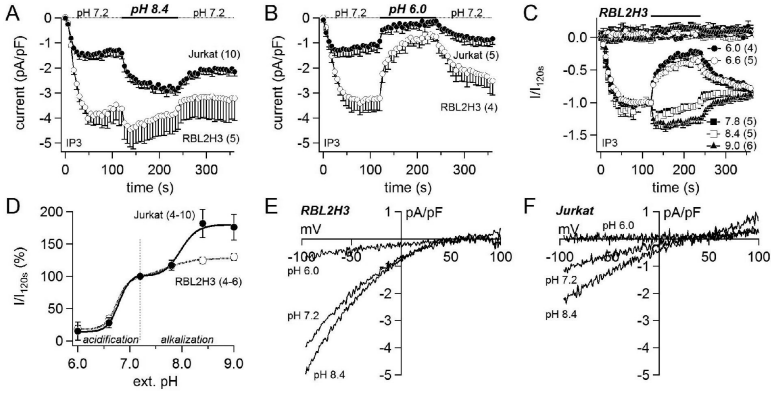

Fig. 1. Extracellular pH modulates endogenous I_{CRAC}

(*A, B*) Averaged time courses of IP_3-induced (20 μM) CRAC currents measured in RBL2H3 cells (open circles) and Jurkat T lymphocytes (filled circles). Inward currents of individual cells were measured at −80 mV, normalized by the cell capacitance, and plotted versus time (-SEM). Bars indicate application of external solution of pH 8.4 (*A*) and 6.0 (*B*). (*C*) Inward and outward currents of RBL2H3 cells, measured at −80 mV and +80 mV, respectively, normalized to the amplitude of the inward current right before pH change (I/I_{120s}), averaged and plotted versus time (±SEM). The bar indicates application of external solution of different pH (6.0 to 9.0). (*D*) Double dose response fits (external pH versus relative change of inward current, I/I_{120s} in %) reveal a pK_a ($pK_{acidification}$) of 6.8 and pK_b ($pK_{alkalization}$) of 8.0 in Jurkat T lymphocytes (closed circles) and a pK_a of 6.7 and pK_b of 7.8 in RBL2H3 cells (open circles). The number in brackets indicates the number of averaged cells. (*E, F*) Typical inwardly rectifying I/V relationships of Ca^{2+}-selective I_{CRAC} at different external pH from RBL2H3 cells (*E*) and Jurkat T lymphocytes (*F*).

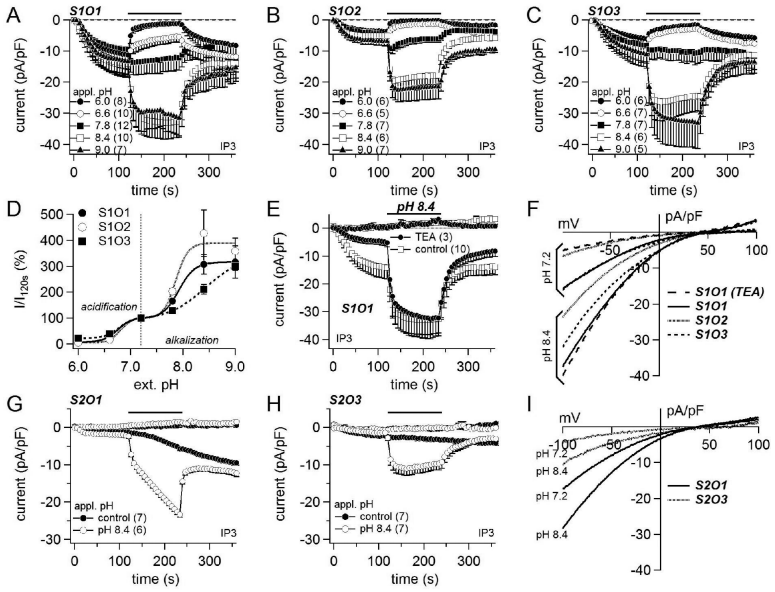

Fig. 2. Extracellular pH modulates heterologous STIM/Orai-mediated I_{CRAC}

(*A, B, C*) Averaged time courses of IP_3-induced (20 μM) CRAC currents measured in HEK293 cells expressing STIM1 and Orai1 (S1O1; *A*), STIM1 and Orai2 (S1O2; *B*) and STIM1 and Orai3 (S1O3; *C*). Inward currents of individual cells were measured at -80 mV, normalized by the cell capacitance, and plotted versus time (-SEM). The bars indicate application of external solution of different pH (6.0 to 9.0). (*D*) Double dose response fits (external pH versus relative change of inward current, I/I_{120s} in %) reveal pK_as ($pK_{acidification}$) of 6.8, 6.8 and 6.7, and pK_bs ($pK_{alkalization}$) of 7.9, 7.9 and 8.4 in S1O1- (filled circles), S1O2- (open circles) and S1O3- (filled boxes) expressing HEK293 cells, respectively. (Same cells as in *A-C*.) (*E*) Averaged time courses of IP_3-induced (20 μM) inward and outward currents, measured at −80 mV and +80 mV, respectively, in S1O1-expressing HEK293 cells in the presence (open boxes) and absence (Na^+ replaced by TEA^+; filled circles) of external sodium. The bar indicates application of external solution of pH 8.4. (*F*) Typical inwardly rectifying I/V relationships of Ca^{2+}-selective I_{CRAC} at different external pH from S1O1-, S1O2- and S1O3-expressing HEK293 cells. The number in brackets indicates the number of averaged cells. (*G, H*) Averaged time courses of IP_3-induced (20 μM) CRAC currents measured in STIM2 and Orai1 (S2O1; G) and STIM2 and Orai3 expressing HEK293 cells (S2O3; H) with (white circles) and without (black circle) application of external solution of pH 8.4.. Inward and outward currents of individual cells were measured at −80 mV and +80 mV, respectively, normalized by the cell capacitance, and plotted versus time (±SEM). (*I*) Typical inwardly rectifying I/V relationships of Ca^{2+}-selective I_{CRAC} in different external pH from S2O1- and S2O3-expressing HEK293 cells at different external pH. The number in brackets indicates the number of averaged cells.

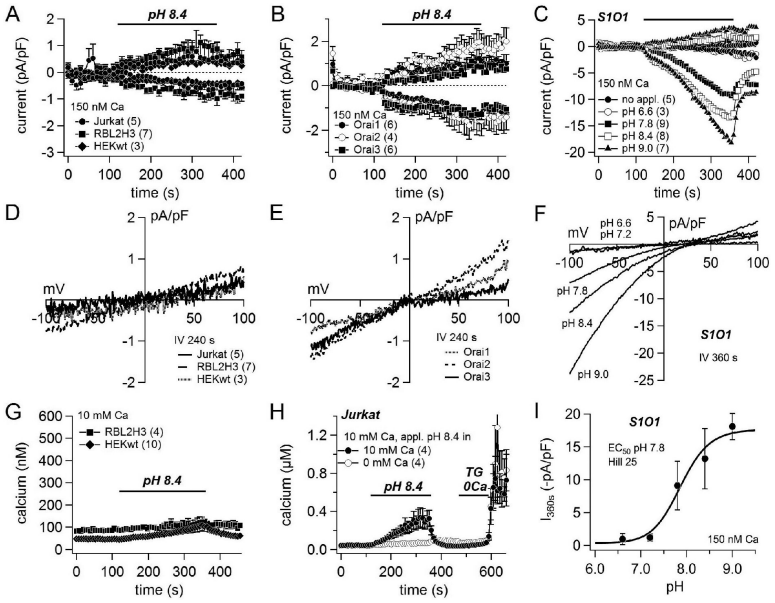

Fig. 3. Extracellular alkalization activates heterologous mediated I_{CRAC}

(*A, B*) Averaged time courses of external pH 8.4-mediated currents measured in HEK293 wild type (HEK wt; filled diamonds), RBL2H3 cells (filled boxes) and Jurkat T lymphocytes (filled circles) (*A*). Orai1-(filled circles), Orai2- (open circles) and Orai3-expressing HEK293 cells (filled boxes) (*B*). Averaged time courses of currents measured in STIM1/Orai1 expressing cells upon application of external solution adjusted to pH values as indicated (*C*). Inward and outward currents of individual cells were measured at -80 mV and +80 mV, respectively, normalized by the cell capacitance, and plotted versus time (±SEM). The intracellular Ca^{2+} concentration was clamped to 150 nM (20 mM Cs·BAPTA + 8 mM $CaCl_2$) to prevent passive store depletion-induced CRAC activation. The bars indicate application of external solution of pH as indicated. (*D, E, F*) I/V relationships corresponding to *A, B* and *C*, respectively. (*G, H*) Averaged time courses of intracellular Ca^{2+} changes due to application of pH 8.4 in intact Fura-2AM-loaded HEK293 wt cells (open diamonds) and RBL2H3 cells (filled boxes) (*G*), and Jurkat T lymphocytes in the absence (open circles) and presence (filled circles) of extracellular Ca^{2+} (*H*). Bars indicate the application of external solution of pH 8.4 or external solution containing 2 µM thapsigargin (TG). (*I*) Dose-dependence of S1/O1-mediated currents induced by external alkalization (EC_{50} pH 7.8). (Same cells as in *C*.) The number in brackets indicates the number of averaged cells.

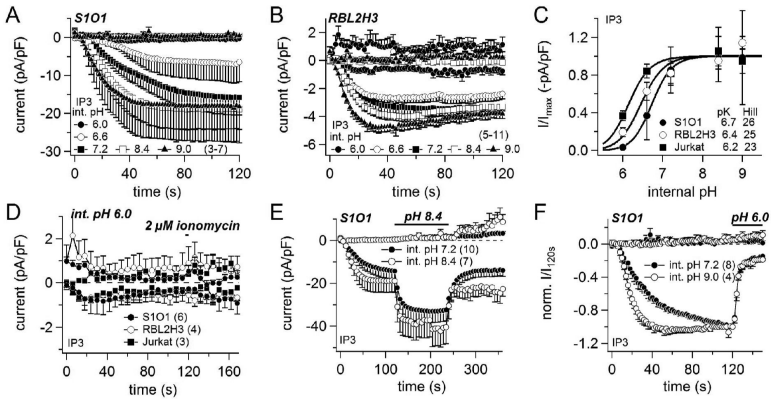

Fig. 4. Intracellular pH modulates IP_3-induced I_{CRAC}

(*A, B, C*) Averaged time courses of IP_3-induced (20 μM) currents measured in HEK293 cells expressing STIM1 and Orai1 (S1O1; *A, C*), RBL2H3 cells (*B, C*) and Jurkat T lymphocytes (*C*) at different internal pH (6.0 to 9.0). Inward and outward currents of individual cells were measured at −80 mV and +80 mV, respectively, normalized by the cell capacitance, and plotted versus time (±SEM). (*C*) Dose response fits (internal pH versus current amplitude, normalized to I_{max}) reveal pKs of 6.7, 6.4 and 6.2 in S1O1-expressing HEK293 cells (filled circles), RBL2H3 cells (open circles) and Jurkat T lymphocytes (filled boxes), respectively. (Same cells as in *A* and *B*.) (*D*) Averaged time courses of IP_3-induced (20 μM) currents measured in S1O1-expressing HEK293 cells (filled circles), RBL2H3 cells (open circles) and Jurkat T lymphocytes (filled boxes) at internal pH 6.0. The bar indicates application of 2 μM ionomycin. The number in brackets indicates the number of averaged cells. (*E*) Averaged time courses of IP_3-induced (20 μM) CRAC currents at internal pH 7.2 (filled circles) and 8.4 (open circles) measured in STIM1 and Orai1 (S1O1)-expressing HEK293 cells. Inward and outward currents of individual cells were measured at −80 mV and +80 mV, respectively, normalized by the cell capacitance, and plotted versus time (±SEM). The bar indicates application of external solution of pH 8.4. (*F*) IP_3-induced inward and outward currents of individual S1O1-expressing HEK293 cells at internal pH 7.2 (filled circles) and 9.0 (open circles), measured at −80 mV and +80 mV, respectively, normalized to the amplitude of the inward current right before pH change (I/I_{120s}), averaged and plotted versus time (±SEM). The bar indicates application of external solution of pH 6.0. The number in brackets indicates the number of averaged cells.

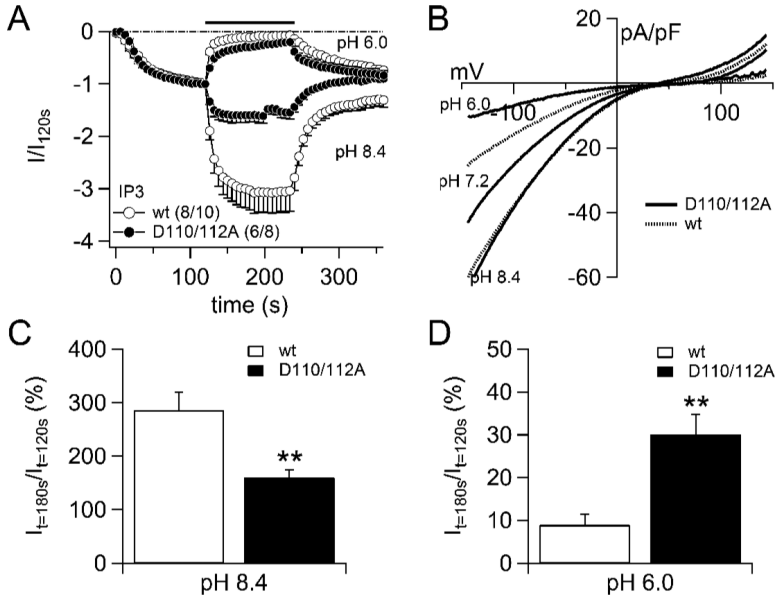

Fig. 5. Contribution of D110 and D112 to pH sensitivity of Orai1

(*A*) Averaged time courses of IP_3-induced (20 μM) CRAC currents measured in HEK293 cells expressing STIM1 and either Orai1 wild type (S1O1; wt) or $Orai1_{D110/112A}$. Inward currents of individual cells were measured at −80 mV. The bars indicate application of external solution of different pH. Currents were normalized to currents at t = 120 s when I_{CRAC} had fully developed and plotted versus time (-SEM). (*B*) I/Vs for cells shown in *A* before application at pH 7.2 and at the end of application (t = 180 s) at pH 6.0 and 8.4. (*C*) Bar diagram for alkalization induced amplification at t = 180 s. Asterisks indicate a significant difference between $Orai1_{wt}$ and $Orai1_{D110/112A}$ (p = 0.003 in a two-sided, unpaired student's t-test). (*D*) Bar diagram for acidification induced residual current. Asterisks indicate a significant difference between $Orai1_{wt}$ and $Orai1_{D110/112A}$ (p = 0.006 in a two-sided, unpaired student's t-test).